Integration of Spatial Modulation Scheme with Code Division Multiple Access for VIVO based Frequency Selective Nano Sensor Networks.

F. Berrahma, K. Ghanem, *Senior Member, IEEE*, H. Bousbia-Salah, A. Alomainy, *Senior Member, IEEE*, M.A. Imran, *Senior Member, IEEE*, Q.H. Abbasi, *Senior Member, IEEE*

***Abstract*— Due to their suitability for human-body based communications, in-VIVO nano sensor networks are envisioned to use the promising Terahertz signals in order to ensure the forthcoming high-rate communication needs of the modern medicine. However, the propagation losses at these frequency bands are quite significant and dependent on the operation frequency as well as on the physiological characteristics, thus impeding the use of Terahertz rates to their utmost benefit. Using numerous emitting elements is likely to improve the quality of the received signal, but gives rise to multi-channel interference (MCI) emanating from multi-antenna signaling reception, which necessitates a relatively complex signal processing to mitigate it. When multiple physiological signals are of interest, detecting them necessitates to mitigate multiple-access interference (MAI). In this perspective, orthogonal frequency division multiplexing (OFDM) allows to combat the channel frequency selectivity, whereas code division multiple access (CDMA) scheme cancels MAI. In this paper, we propose to embed the novel spatial modulation technique with CDMA architecture in an OFDM framework to ensure a viable communication in in-VIVO frequency selective Nano channels. The immunity of our proposed solution to such an interference is confirmed, since less than -2 dB in SNR level is required to support 5 users simultaneously communicating with a BER which is inferior to 10^{-3} when the operating frequency is equal to 1THz. This hybrid scheme is shown to efficiently combat the MCI while enabling a safe retrieval of the useful signal at the very-high data rate communications.**

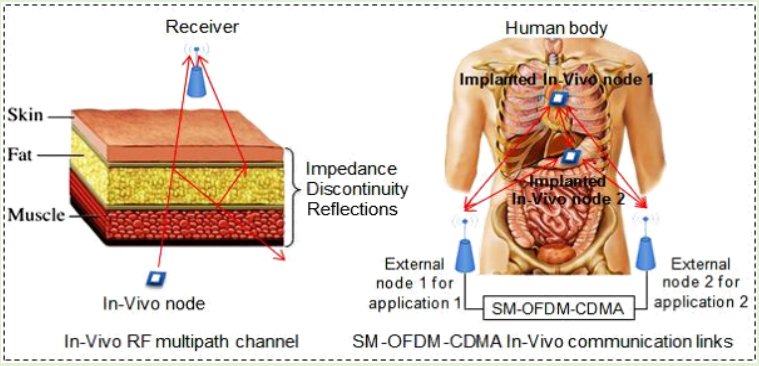

***Index Terms*— Spatial modulation, OFDM, CDMA, in-VIVO nano sensor networks, THz frequencies.**

I. Introduction

IT has become obvious that, unless the frequency resources allocation policy is totally reviewed to encompass the cognitive radio paradigm, in which the primary users share their bands with the secondary users, the frequency resources in low and medium bands are used to their extreme, and can no more support additional subscribers. Under this perspective, the free terahertz (THz) systems are considered as the alternative to allow the ultra-high data rates communications foreseen for the forthcoming sixth generation (6G) of wireless systems.

Incorporating technological tools in the biomedical field has allowed the consolidation of the medical care quality, the decrease of care costs and the increase of human life expectancy. In-VIVO Wireless body area networks (WBANs) and technologies, such as wireless capsule endoscopes and nerve simulators, are no exception, and are likely to be widely adopted in future biomedical services and infrastructures. Indeed, they are oriented towards the same trend of ensuring ubiquitous health monitoring, assisting the doctors in delivering reliable and accurate diagnosis and analysis, screening early critical diseases, and offering the patients a seamless physiological data collection and the comfortable idea that the surgery will be avoided unless it becomes the ultimate solution.

In monitoring a patient's real-time vital signs through WBAN technology, rich data sources are communicated to medical

Fadila Berrahma and Hicham Boussbia-Salah are with the National Polytechnic School (ENP), El Harrach, Algiers, Algeria (email: fadila.berrahma@g.enp.edu.dz, hicham.bousbia-salah@g.enp.edu.dz)

Khalida Ghanem is with the Center for Development of Advanced Technologies,CDTA, City 20 aout 1956 Baba Hassen, Algiers, Algeria(e-mail: kghanem@cdta.dz)

Akram Alomainy is with the Antennas and Electromagnetics Group, School of Electronic Engineering and Computer Science, Queen Mary, University of London, London E1 4NS U.K. (e-mail: a.alomainy@qmul.ac.uk)

Muhammad Ali Imran and Qammer Hussain Abbasi are with the Department of Electronics and Nanoscale Engineering, University of Glasgow, and Glasgow, UK(e-mail: Muhammad.Imran@glasgow.ac.uk, Qammer.Abbasi@glasgow.ac.uk)

practitioners. Beyond clinical use, professional disease management environments, and private personal health assistance scenarios (without financial reimbursement by health agencies/insurance companies), WBAN enables a wide range of health care applications and related services. In [1], the authors propose a non-intrusive breathing monitoring system using the C-Band sensing technique. In [2], cooperative techniques are exploited to enhance the coverage and the reliability of WBANs. Interference cancellation in WBANs is targeted in [3], while [4] introduces an FPGA-based realistic solution to reduce the implementation complexity by recoursing to compressed sensing tools. Recently, the nanotechnology and the subsequent possibilities it opens for the reduction of the devices size to the nanoscale dimension, in addition to the research community interest for the adequate nano materials for such devices, such as the graphene, have made conceivable the adoption of the nano-networks for the THz communication within the human body. However, one major problem faced with the deployment of this breakthrough technology, in addition to the very high path loss and molecular absorption noise, is the resulting high level of multiuser interference. This latter comes from the very high density of in-body sensors; in the order of hundreds per square millimeter, which needs to be deployed in order to compensate the reduced coverage range, pertaining to the operation at the THz band. The signals emanating from the co-communicating transmitters at the reception side are superimposed with the signal of interest, leading to the degradation of the communication quality. The investigation of the body-supported networks has been thouroughly carried out in the last two decades, at the ISM and UWB frequencies [3], [5]–[11]. The characterization of the propagation and the channel modeling of the THz in-vivo networks have been recently conducted in [12]–[15]. According to the authors knowledge, only few studies have been accorded to these particular networks, when evolving in multi-user scenario. The authors in [16], [17] proposed a pulse communication-based statistical interference model which is adapted to THz-band in a very specific setting. The weakness of that work lies in the fact that the presented interference model, relying on the polynomial approximation of the received signal, is parametrized by the power and shape of the transmitted signal and the channel molecular distribution, hence varies with the variation of the communication medium or the signal features. Interference and signal-to-noise-plus-interference ratio (SINR) was also analyzed in [18]–[20] when considering the effect of antenna radiation pattern and directivity. In [21], a network level analysis was carried out by extracting the interference model and the SINR of the in-VIVO nano-networks when adopting time spread ON-OFF keying (TS-OOK) modulation scheme was derived. Various communication conditions were investigated to highlight the interference impingement on signal degradation. According to the discussion above, it appears clearly that the previous studies have solely been concerned with assessing the effect of interference on the THz communication of the nano networks. Surprisingly, no work has been dedicated to overcoming this undesirable effect. Motivated by this limitation, in this paper, a solution is proposed to mitigate interference in this particular environment, by recoursing to a scheme which combines index modulation and code division multiple access. The adoption of the index modulation is consolidated by the current communication trend in its incorporation in massive multiple-input multiple-output (MIMO) systems. Indeed, a key challenge of future mobile communications research is to strike an attractive compromise between the two wireless network's areas: spectral-efficiency and energy-efficiency. This necessitates a clean-slate approach to wireless system design, embracing the rich body of the existing knowledge on MIMO technologies to its extension to massive MIMO paradigm [22], [23]. However, conventional MIMO systems design would need an RF chain at each transmitting and receiving element side, rendering the integration of massive MIMO, practically unfeasible due to the high hardware complexity and the prohibiting energy consumption. To alleviate such constraints, index modulation, which in spatial domain holds the name of spatial modulation (SM), has emerged as a viable solution in 5G and beyond-communication systems, and proposed to include within the transmitted signal block, a part dedicated to the activated antenna index, in addition to the usual data part [24], [25]. This allows to circumvent in the uplink single user scenario, and without resorting to successive interference cancellation (SIC) schemes, the inter-channel interference (ICI) emanating from multiple transmitting antennas to the same receiver. This is achieved in the conventional SM scheme by randomly activating only one antenna at the transmit side, and retrieving from the signal block at the multiple-antennas receive side both the index of the activated antenna and the associated transmitted data. Most of the SM-related contributions have addressed point-to-point communication systems, i.e. the case of the single-user, and the investigated channels were undergoing mostly either flat Gaussian or flat Rayleigh fading [26]. According to the best of our knowledge, the sole work incorporating index modulation for in-VIVO nano networks has targeted a single device scenario [27]. Furthermore, a very little research interest has been dedicated to the investigation of SM architectures in multiple user access context, and the ones which have reported related works, have only dealt with flat fading channels [28], [29]. The objective of this work is to address the realistic scenario of the dense deployment of numerous nano-sensors within the human body, and propose a scheme combating the effect of path loss and multiple access interference in THz frequencies. Obviously, in upcoming communication multipoint-receive systems, in addition to the challenging targeted types of applications where high data rates and mobility are involved, the pertaining solutions should support a large number of receive devices, while maintaining the required quality of service (QoS) per device, and keeping the hardware complexity as simple as possible. Due to the involved large communication frequency band and high data rates, the associated in-body channel will be shown to be frequency-dependent. In this direction, we have retained orthogonal frequency division multiplexing (OFDM) to combat the THz channel frequency selectivity. OFDM technique achieves such purpose, by converting the selective channel into a set of frequency-flat subchannels, which number is equal to the number of subcarriers used

in the OFDM scheme. Furthermore, code division multiple access (CDMA), consisting in assigning a different code per targeted transmit device, allows to support multiple access in SM architectures. We agree, to refer, in the MIMO in-VIVO setting, to the interference at the receiver emanating from the multiple transmitting antennas of the intended physiological signal as ICI. Similarly, the one originated from a transmitting device other than the intended signal is conventionnally termed as multiple access interfernce (MAI). The combination of OFDM, SM and CDMA techniques, targetting to increase the data rate, while mitigating the ICI and the MAI in THz frequency selective channel, gives birth to the new concept of SM-OFDM-CDMA. The paper is organized as follows. Section II introduces the proposed channel model. Section III details the proposed hybrid spatial modulation scheme. Numerical results are provided in Section IV and finally, conclusions are drawn in section V.

II. Channel Characterization and Modeling

The in-VIVO THz channel is challenging to characterize and estimate but has attracted lately the research interest because of the development witnessed in nanotechnology and device miniaturization. The in-body electromagnetic waves at the THz band cross different media wihin the human body, each with different electrical and magnetic properties. In this work, we represent the skin tissues, as shown in Fig.1, by a three-layer model, namely the stratum corneum (SC), the epidermis, and the dermis.

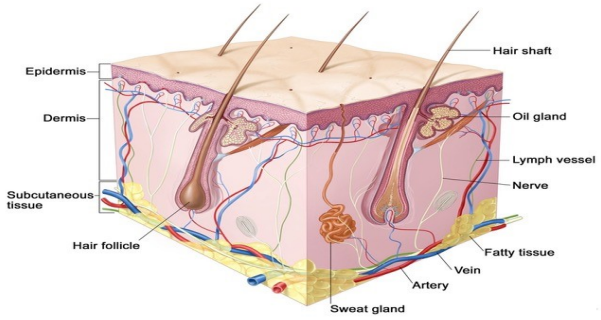

Fig. 1. Representation of skin tissues.

To accurately emulate the electromagnetic propagation inside the human tissues and the resulting losses they generate within a given signal, the epidermis region was supposed containing sweat glands or sweat ducts, which are of spiral shape. We have developed a large scale model in [15] and validated it through time-domain spectroscopy (THz-TDS) experiments carried out at Queen Mary University of London (QMUL) [30] by using two layers, the epidermis extracted from a real being skin, and an artificially cultured collagen emulating the dermis. The collected phase and amplitude of received pulses are processed via transfer equation-based algorithm, which allows the evaluation of the pathloss and other material parameters [31]. For readers interest, more details on the system setup and performed measurements could be found in [15]. The modified Friis equation proposed in [12] which evaluates the path loss in the water vapor channel at the THz band considers two phenomenons, namely the expansion of electromagnetic (EM) waves in the tissue giving rise to the spreading path loss (PL_{spr}), and absorption of the waves in the tissues producing the absorption path loss (PL_{abs}). Accordingly, the path loss in the human tissues could be written as:

$$PL_{total}[dB] = PL_{spr}(f,d)[dB] + PL_{abs}(f,d)[dB] \quad (1)$$

where f refers to the frequency in THz, and d to transmitter-receiver distance expressed in millimiters. However, this slow fading model is concerned only with the frequency and distance operation parameters, and overlooks the physiological particularities of the internal part of the human skin. This was taken into account in the model we developed in [15] inferred from the THz-TDS skin measurements, and encompassing the number of sweat ducts in the skin. Unlike our previous works, we are targeting herein a MIMO configuration, and we define our path loss model in each l^{th} multipath signal component between each j^{th} receive antenna and i^{th} transmit antenna of the in-body nano nodes, by complying with the two-step data fitting procedure with the measurements, which yields the following model:

$$PL^{l}_{j,i} = -0.2 * N + 3.98 + (0.44 * N + 98.48) d^{0.65}_{j,i} + (0.068 * N + 2.4) f^{4.07} \quad (2)$$

with N being the number of sweat ducts and $l = \{1, 2, ..., L\}$ indicates the number of multipath channel components. In the following, the impingements of the characteristics of the nano-scale in-body environment, the operation frequency and the inter-nodes distance on the channel path loss are investigated, and the obtained results are illustrated in Fig.2 through Fig.4. According to Fig.2, it appears that the variation of the number

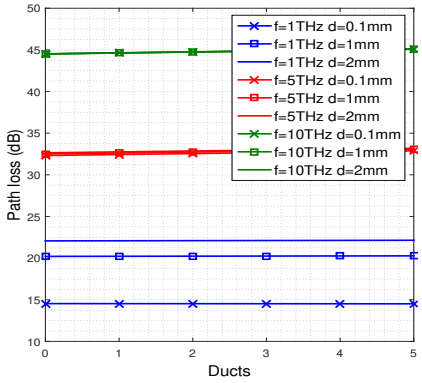

Fig. 2. Path loss with respect to the number of ducts

of ducts in the chosen range has a negligeable effect on the path loss, whatever the operation frequency is. Hence a displacement from an in-body area to a neighbouring region does not induce an appreciable variation in the path loss. At a given number of ducts, increasing the transmitting-receiving elements distance results in a path loss increase at f=1THz, unlike the other frequency of interest, i.e. f=5THz and f=10THz, at which the same path loss is attained, regardless of the distance. On the other hand, Fig.3 shows the path loss

in terms of the distance for different numbers of ducts and frequencies. From that figure it appears that the path loss observed when varying the distance is the same, regardless of the number of ducts. Furthermore, the increase of the operating frequency results in a higher path loss. When f=1THz, and up to a distance of 1mm, the path loss scales linearly with the variation of the distance, and a small variation of the distance by an order of 0.1mm results in approximately 1dB increase of the path loss. Beyond this value, the path loss at f=1THz is only slightly affected by the distance. For the other higher frequencies of interest, the path loss is not impinged by the distance at the investigated range.

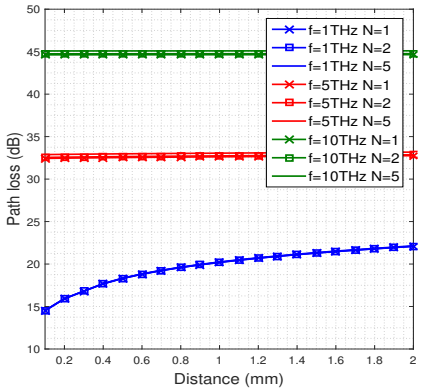

Fig. 3. Path loss with respect to the distance

Finally, the effect of the operation frequency on the path loss is addressed and the corresponding results are reported in Fig. 4. As it can be noted, the path loss remains constant at 22 dB when the frequency is below 2 THz. After this threshold, the path loss increases almost linearly by a step of 5 dB at each 1 THz-frequency increase.

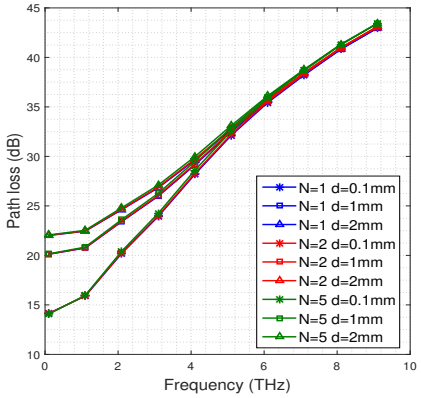

Fig. 4. Path loss with respect to the frequency (f)

III. Hybrid Spatial Modulation Scheme with CDMA Multiple Access

Our scenario involves numerous nano-sensors placed within the body, where each, to comply with hardware and energy constraints, is equipped with a sole antenna. Subsets of them are regrouped to form virtual MIMO configurations, where each of those is dedicated to a given application (physiological data), referred to herein as user, thus forming a multiuser system. Index modulation scheme conveys additional information in the data block beside the transmitted symbol, which can be an index of the temporal, spatial, or the frequency resource activated for such a transmission. In this work, the index pertains to the spatial dimension, leading to the particular case of SM. By randomly activating only one antenna, the ICI is mitigated and the only remaining interference is the MAI coming from the co-existence of multiple physiological signals (users) sharing the same frequency and temporal resources and co-communicating with the same reception unit. This MAI will be reduced by resorting to CDMA scheme. Indeed, these spatially distributed nano-networks, are virtually regrouped such that to use N_t nano transmit nodes for a given application, and K users (referring to different applications or different physiological signals) are simultaneously communicating with the receive unit consisting of N_r distributed receive nodes. Figure 5 shows an example of SM-OFDM scheme with $N_t = 2$ and 4 OFDM sub-carriers, and which adopts 4QAM modulation resulting in 3bits/symbol/sub-carrier transmission. The SM-OFDM information block pertaining to each subcarrier is mapped into the index of the activated transmit antenna and the emitted symbol. Let us assume for instance that the input data sequence corresponding to the first sub–carrier is $[0 \quad 1 \quad 1]^T$. Since we are concerned with only two transmit antennas, the first element in the information block (the value zero herein) refers to the antenna index, while the remaining elements are the data block. Hence, this example corresponds in SM mapping to the transmission of the symbol $1 - i$ from the first transmit antenna while at that time instant the second antenna is kept silent. Hence, the transmit symbol vector for the first sub-carrier is $[1 - i \quad 0]^T$. The block

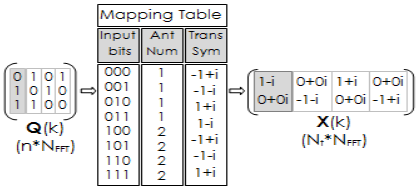

Fig. 5. SM-OFDM: 3bits/symbol/subcarrier in 4QAM modulation.

diagram of the used architecture is shown in Fig.6. At the transmitter side, the input data sequence $\mathbf{d}(k)$ corresponding to the k^{th} biophysical signal is first encoded, interleaved and then inserted into the SM block to generate the sequence $\mathbf{q}(k)$. Hence, in the SM architecture, the first $log_2 N_t$ of the resulting block are dedicated to the coding of the antenna index, while the second $log_2 M$ bits contains the emitted symbol. Therefore, the number of bits/symbol per user that this SM scheme allows to transmit in each block is given as presented in [24]:

$$b_{SM} = log_2 N_t + log_2 M \tag{3}$$

In each k^{th} application-dedicated system, $k = \{1, ..., K\}$, the signal vector $\mathbf{x}(k)$ is CDMA-spread by performing the Hadamard product between an array of the signal $\mathbf{q}(k)$ repeated N_t times and the spreading code $\mathbf{c}^{(k)} \in \mathbf{C}^{N_t \times P}$ [32].

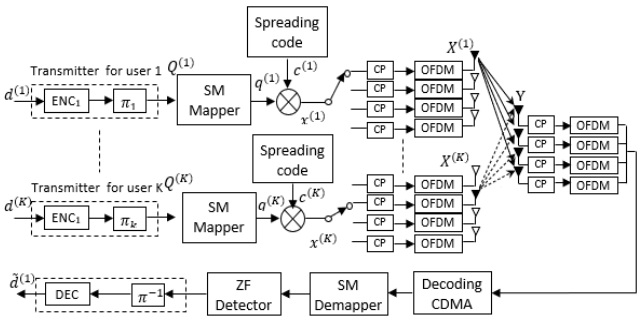

Fig. 6. SM-CDMA-OFDM system transceiver block diagram.

Hence the CDMA encoded signal could be written as:

$$\mathbf{x}^{(k)} = \mathbf{q}^{(k)}. \quad \mathbf{c}^{(k)} \in \{-1, +1\}^{1\times P} \tag{4}$$

with P being the length of the spreading code. Afterwards, in each transmitter, the input sequence is transformed to the time domain by applying the inverse fast Fourier transform (IFFT). Subsequently, a cyclic prefix (CP) is inserted to eliminate the inter-symbol interference (ISI) between OFDM symbols, and the resulting signals are transmitted over the channel. The multipath signal received at the ϱ^{th} antenna element from transmit antennas could be written as:

$$\mathbf{y}_{\varrho}(t) = \sum_{i=0}^{K} \mathbf{h}_{\varrho\nu}(t) \otimes \mathbf{x}_{\nu}(t) + \mathbf{w}_{\varrho}(t) \tag{5}$$

where $\mathbf{x}_{\nu}(t)$ is the signal emanating from the ν^{th} activated antenna, $\mathbf{w}_{\varrho}(t)$ is the additive white Gaussian noise vector with $CN(0, \sigma^2)$ elements, $\otimes$ denotes the time convolution operator and $\mathbf{h}_{\varrho\nu}(t) = \begin{bmatrix} h_{\varrho\nu}(t)^1 & h_{\varrho\nu}(t)^2 \cdots h_{\varrho\nu}(t)^L \end{bmatrix}$ stands for the $L \times 1$ channel vector between the pair of ν^{th}transmit-ϱ^{th}receive antennas encompassing the L significant multipath channel components. The receiver at the branch corresponding to the retrieval of the k^{th} user signal, as illustrated in Fig.6, comprises simply the blocks performing the reverse ordered operations of the transmitter side. First, OFDM demodulation is carried out, then, the resulting signal is multiplied by the CDMA code associated with the k^{th} application, and summed up such that to re-obtain the despread signal. Then, the SM decoding operation is launched by estimating the index of the activated antenna from the signal block part reserved to the indices, and then demodulating the associated signal using zero forcing (ZF) detector; which is viewed as an element-wise division of the OFDM demodulated signal by the transfer function of the discrete channel response. The so-mentioned channel transfer function is computed by a DFT of the zero-padded discrete time channel impulse response. It follows that the per-carrier ZF is performed as described in [33]:

$$\tilde{\mathbf{z}}^{s}(k) = \frac{\mathbf{y}^{s}(k)}{\mathbf{h}_{j}^{s}(k)} \tag{6}$$

where s stands for the index of the subcarrier. Afterwards, spatial location of the transmit antenna index, from which the symbol was transmitted, needs to be estimated. This is done by finding the location of the maximum absolute value of the output vector from the ZF equalizer $\tilde{\mathbf{z}}(k)$ for each sub-carrier s, which is described in the following equation:

$$\hat{j} = arg\max_{j} |\tilde{\mathbf{z}}^{s}(k)| \; for \; j = \{1, 2, .., N_t\} \; s = \{1, 2, .., FFT\} \tag{7}$$

where $\hat{j}$ denotes the estimated value of the antenna index. Then, the symbol is detected using the following equation:

$$\hat{q} = Q(\tilde{\mathbf{z}}^{s}(k)_{(j=\hat{j})}) \tag{8}$$

where Q refers to the quantization operation pertaining to the symbol detection. After the SM-OFDM demapping, decoding and de-interleaving operations are applied, as shown in the Fig.6.

IV. Simulation Results

To study the performance of the proposed multiple access spatial modulation scheme incorporating virtual MIMO-OFDM configuration in the in-VIVO THz channel, simulations are carried out to study the impact of different parameters on such a performance. In the following, we comply with the

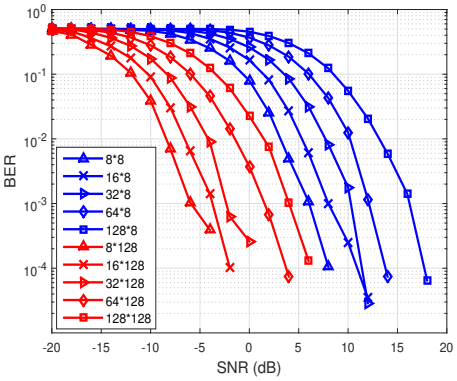

Fig. 7. Comparison of BER performances of SM-OFDM-CDMA scheme with the variation of transmit and receive antenna numbers with f=1THz, $\mathbf{2PSK, FFT = 128, N_c = 128, N = 1, d = 0.1mm}$

SM notation adopted in multiple papers when referring to the resulting MIMO system adopting M-PSK modulation, i.e. $N_t \times N_r$ M-PSK. We next analyze the effect of transmit and receive antenna (TX-RX) number on the BER performance, with: $N_t = \{8, 16, 32, 64, 128\}$ and $N_r = \{8, 128\}$, whereas the length of the spreading CDMA code (N_c) and the number of subcarriers (FFT) are fixed at 128, and 2PSK modulation is retained. As depicted in figure 7, the performance significantly improves when increasing the number of receive antennas. However, this same performance degrades when the number of transmit antennas is greater than the number of receive antennas. This consolidates the finding in papers [34]–[36], where it was shown that the transmit antenna index is better detected and accurately estimated in the presence of a lower number of TX-antennas than the receive ones. It follows that for the investigated cases, the best performance is achieved when $N_t = 8$ and $N_r = 128$.

Fig. 8 investigates the BER performance when fixing the spectral efficiency per subcarrier, as given by the expression

in Eq. 3, at the value 9 bits/s/Hz, for instance. This is achieved by increasing the order of the modulation from 2 to 128 PSK, with a power of 2, while decreasing the number of transmit antennas, such that to maintain the spectral efficiency constant, as per Eq. 3. It can be seen from Fig. 8 that the higher modulation orders, such as 64 PSK and 32 PSK, experience a quite acceptable penalty in terms of data reliability thanks to the balance provided by a number of transmit antennas which is below the one of receive antennas. On the other hand, the schemes incorporating the lower modulation orders, i.e 4 PSK and 8 PSK, exhibit performances which are below the ones expected due to a corresponding numbers of transmit antennas that are close to receive antennas. The scheme which yields the best compromise between the number of transmit antennas and the modulation type is the one supporting 16 PSK, resulting in the best performance.

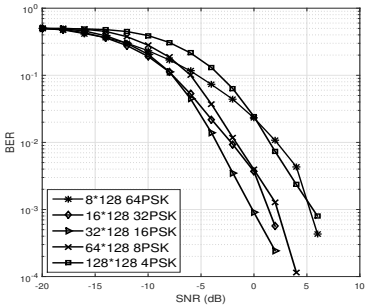

Fig. 8. Comparison of BER performances of SM-OFDM-CDMA scheme with the variation of the modulation order M, f = 1THz, $\boldsymbol{FFT = 128, N_c = 128, N = 1, d = 0.1mm}$

In next simulation the impingement of the variation of the number of subcarriers on the performance of the proposed system is investigated when the operating frequency is f=1THz, $(N_t, N_r) = (8, 128)$, the 2 PSK modulation is adopted and the distance is maintainted at d=0.1mm. As expected, increasing the number of subcarriers corresponds to affording more parallel frequency branches to transmission, hence enhancing the frequency diversity. It follows that the BER performance is significantly enhanced; for instance migrating from a system supporting 32 subcarriers to a one supporting 128 allows reducing the SNR by more than 5 dB at a required BER of 10^{-3}. The performance of the proposed systems is discussed

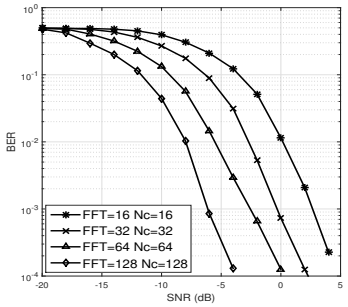

Fig. 9. Comparison of BER performances of SM-OFDM-CDMA scheme with the variation of FFT size and $\boldsymbol{N_c}$ at $\boldsymbol{N_t = 8, N_r = 128, N = 1}$, f=1THz, $\boldsymbol{d = 0.1mm}$

in the same setting when varying the number of subcarriers and the operating frequencies, and the associated results are illustrated in Fig. 10. As mentioned earlier, the impact of the operation frequency on the performance is the most critical compared to other parameters. Indeed, increasing the frequency from f = 1THz to 5 THz, induces an approximate penalty of 20 dB in terms of SNR and of more than 10 dB when migrating from 5THz to 10THz. Moreover, for a given operation frequency, increasing the number of carriers from 64 to 128 results in an average gain of 3 dB in terms of performance. Next, the effect of multiple access interference

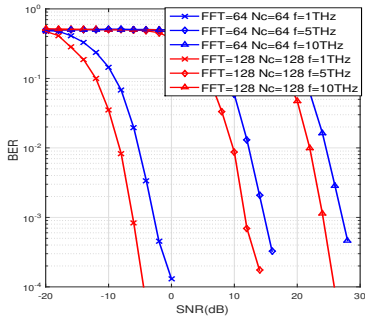

Fig. 10. Comparison of BER performances of SM-OFDM-CDMA scheme with the variation of FFT size and $\boldsymbol{N_c}$ at $\boldsymbol{N_t = 8, N_r = 128, N = 1}$, $\boldsymbol{d = 0.1mm}$ and different frequencies.

on the performance of the proposed solution is of interest. For this purpose, the parameters are chosen as follows: the number of users (corresponding to different physiological signals) is varied as $K = \{1, 2, 5\}$, the operating frequency is selected from the set $f = \{1, 5, 10\}$THz, the Tx-Rx distance is maintained at 0.1mm, and the remaining parameters are fixed at $(N_t, N_r, M, FFT) = (8, 128, 2, 128)$. Moreover, for simplification purposes, the length of the spreading CDMA code is $N_c = 128$, and we have incorporated in each frame only one OFDM block. As it can be seen from Fig.11, the

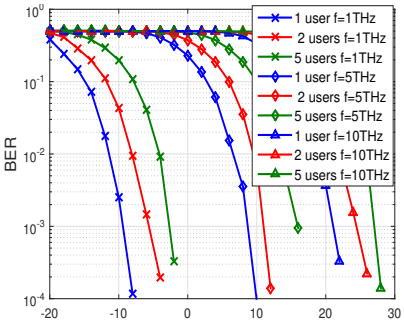

Fig. 11. Comparison of BER performances of SM-OFDM-CDMA scheme with the variation of the number of users $\boldsymbol{N_t = 8, N_r = 128, 2PSK, FFT = 128, N_c = 128, N = 1}$, $\boldsymbol{d = 0.1mm}$ and different frequencies

reliability of the data at a given frequency is degraded by the users number increase, which is what was expected. For instance, moving from a scenario supporting only 1 user to the one containing 5 users results in an approximate penalty

of 7 dB in terms of SNR. Operating at the lowest frequencies of the terahertz band seems to be more interesting in practice, because of the cost of the higher ones in SNR increase. The balance of this at those high frequency range could be achieved by significantly increasing the number of subcarriers, at the price of a more significant hardware complexity. At f= 1THz, the immunity of our proposed solution to such an interference is confirmed, since less than -2 dB in SNR level is required to support 5 users simultaneously communicating with a BER which is inferior to 10^{-3}. In the following, the effect of the variation of the physiological media is studied at a transmitter-receiver distance of 0.1 mm and a frequency chosen from the set f= {1, 5, 10 }THz in the presence of a MAI level consisting of five users, and the pertaining results are reported in Fig.12. As observed, it is again shown that the achievable performance for a given frequency, is independent of the media in which the communication scheme is embedded, for the ones incorporating a number of ducts ranging from 1 to 5. This consolidates the results reported in Fig.2 through Fig. 4, where the path loss is shown to be the same regardless the number of ducts. Figure 13 discusses the extent of the impact

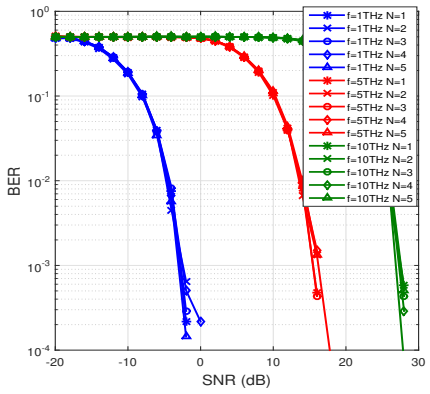

Fig. 12. Comparison of BER performances of SM-OFDM-CDMA scheme with the variation of the number of ducts $\boldsymbol{N_t = 8, N_r = 128, 2PSK, FFT = 128, N_c = 128, d = 0.1mm}$, five users and different frequencies

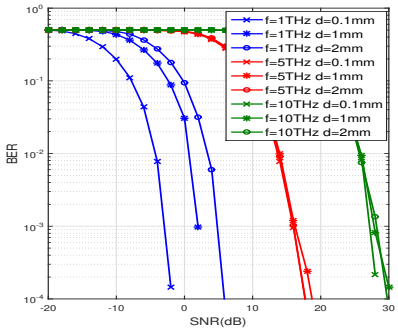

Fig. 13. Comparison of BER performances of SM-OFDM-CDMA scheme with the variation of the distance $\boldsymbol{N_t = 8, N_r = 128, 2PSK, FFT = 128, N_c = 128}$, N=1, five users and different frequencies

of the transmitter-receiver distance on the quality of reception, in the presence of MAI and when the operation frequency is varied in the set f= {1, 5, 10 }THz and the number of co-communicating users is 5. Similarly to the trend seen in Fig .2 and .3, it is demonstrated that the BER performance in the presence of MAI is sensitive to the distance only at the lower range of THz frequencies. At 5 THz and 10 THz frequencies, the performance is very slightly impacted by the distance. At 1 THz, in order to ensure the required BER value of 10^{-3}, an additional SNR of 6.5 dB is necessary when moving the receiver from d=0.1 mm to 1 mm apart from the transmitter. In Fig.14, the achievable performance of the proposed 2PSK-supporting scheme in terms of the frequency of operation and the number of receive antennas is addressed in the presence of MAI. To carry out this study, the number of users is 5, the number of ducts is 1, and the distance is d=0.1mm. As observed, the reliability of the data is altered by the RX number decrease what ever is the used frequency, which is what was expected. However, the most important issue

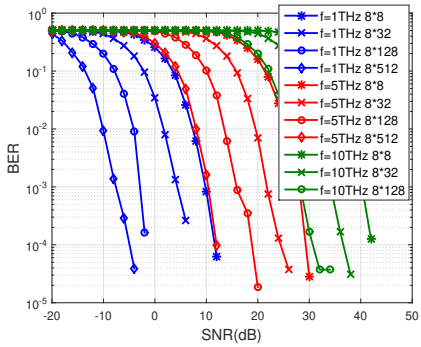

Fig. 14. Comparison of BER performances of SM-OFDM-CDMA scheme with the variation of the number of receive antennas $\boldsymbol{N_t = 8, 2PSK, FFT = 128, N_c = 128, N = 1, d = 0.1mm}$ and five users

is that, despite the high level of co-supported and acquired physiological signals, i.e. 5 in this case, decreasing the transmit antenna number and increasing that of receive antennas allows to enhance the BER performance, regardless of the opertaing frequency. This consolidates again the statement of SM better performance when the number of receive antennas exceeds the transmit antennas.

V. Conclusion

The main objective of this work was to propose an architecture based on spatial modulation which meets the requirements of future generations of health mobile networks, in terms of quality of service and system complexity, while ensuring multiple signal acquisition in in-VIVO Nano networks. It was shown that to ensure a better performance and signal retrieval at the reception, the number of transmit antenna should be less or equal to the number of receive antennas. Furthermore, because of the in-body channel sensitivity to the high frequencies in the terahertz band, the reliability of the received data is altered. Hence, unless it becomes necessay the lower range of terahertz band should be targeted, and otherwise endow the system with a higher number of subcarrier branches to ensure a more performant OFDM signaling. The impact of the physiological media reflected by the number of ducts was

demonstrated to be negligible at these frequencies and the transmitter-receiver element distance was also shown to be of importance only at lower frequencies. The robustness of the resulting architecture to the multiple access and multipath fading interferences has been confirmed. The number of different influential signals (users) has been maximed at 5, which is a reasonnable assumption, however the ambient noise was assumed to be Gaussian. A more accurate distribution of that may bring a new insight towards the incorporation of advanced wireless communication nanonetworks within the body. A new scheme combining SM-OFDM and CDMA is proposed inside the human skin at terahertz frequencies by considering different distances, number of sweat ducts and frequencies, combating strongly the effect of path loss and multiple access interference and keeping the hardware complexity as simple as possible at a required quality of service (QoS). Hence, the reported analysis highlights the novel method to cater the communication challenges in such environment and paved a way for further studies in this harsh environment, for healthcare applications.

REFERENCES

[1] X. Yang, D. Fan, A. Ren, N. Zhao, and M. Alam, "5g-based user-centric sensing at c-band," *IEEE Transactions on Industrial Informatics*, vol. 15, no. 5, pp. 3040–3047, 2019.

[2] B. Amouri, K. Ghanem, and M. Kaddeche, "Hybrid relay selection-based scheme for uwb bans combining mb-ofdm and decode-and-forward cooperative architectures," *Electronics Letters*, vol. 52, no. 24, pp. 2017–2019, 2016.

[3] K. Ghanem, P. Hall, and R. Langley, "Interference cancellation in body-area networks using linear multiuser receivers," *International Journal of Wireless Information Networks*, vol. 17, no. 3, pp. 126–136, 2010.

[4] O. Kerdjidj, A. Amira, K. Ghanem, N. Ramzan, S. Katsigiannis, and F. Chouireb, "An fpga implementation of the matching pursuit algorithm for a compressed sensing enabled e-health monitoring platform," *Microprocessors and Microsystems*, vol. 67, pp. 131–139, 2019.

[5] K. Ghanem, I. Khan, P. Hall, and L. Hanzo, "Mimo channel modeling and capacity of body area networks," *IEEE Trans. Antennas Propag.*, vol. 60, no. 6, pp. 2980–2986, 2012.

[6] K. Ghanem and P. S. Hall, "Power and bit allocation in on-body channels using mimo antenna arrays," *IEEE transactions on vehicular technology*, vol. 62, no. 1, pp. 404–408, 2012.

[7] ——, "Interference cancellation using cdma multi-user detectors for on-body channels," in *2009 IEEE 20th international symposium on personal, indoor and mobile radio communications*. IEEE, 2009, pp. 2152–2156.

[8] K. Ghanem, "Effect of channel correlation and path loss on average channel capacity of body-to-body systems," *IEEE transactions on Antennas and propagation*, vol. 61, no. 12, pp. 6260–6265, 2013.

[9] M. El Azhari, M. Nedil, Y. S. Alj, I. B. Mabrouk, K. Ghanem, and L. Talbi, "Off-body los and nlos channel characterization in a mine environment," in *2015 International Conference on Electrical and Information Technologies (ICEIT)*. IEEE, 2015, pp. 114–118.

[10] M. E. H. El Azhari, M. Nedil, I. B. Mabrouk, K. Ghanem, and L. Talbi, "Characterization of an off-body channel at 2.45 ghz in an underground mine environment," *Progress In Electromagnetics Research M*, vol. 43, pp. 91–100, 2015.

[11] W. Dib, K. Ghanem, M. Radi, F. Z. Bouchibane, and A. Maali, "An experiemental system-based analyis of humain body motions using embedded sensors," in *2014 IEEE Antennas and Propagation Society International Symposium (APSURSI)*. IEEE, 2014, pp. 981–982.

[12] J. M. Jornet and I. F. Akyildiz, "Channel modeling and capacity analysis for electromagnetic wireless nanonetworks in the terahertz band," *IEEE Transactions on Wireless Communications*, vol. 10, no. 10, pp. 3211–3221, 2011.

[13] K. Yang, A. Pellegrini, A. Brizzi, A. Alomainy, and Y. Hao, "Numerical analysis of the communication channel path loss at the thz band inside the fat tissue," in *2013 IEEE MTT-S International Microwave Workshop Series on RF and Wireless Technologies for Biomedical and Healthcare Applications (IMWS-BIO)*. IEEE, 2013, pp. 1–3.

[14] P. Boronin, D. Moltchanov, and Y. Koucheryavy, "A molecular noise model for thz channels," in *2015 IEEE International Conference on Communications (ICC)*. IEEE, 2015, pp. 1286–1291.

[15] Q. H. Abbasi, H. El Sallabi, N. Chopra, K. Yang, K. A. Qaraqe, and A. Alomainy, "Terahertz channel characterization inside the human skin for nano-scale body-centric networks," *IEEE Transactions on Terahertz Science and Technology*, vol. 6, no. 3, pp. 427–434, 2016.

[16] J. M. Jornet and I. F. Akyildiz, "Low-weight channel coding for interference mitigation in electromagnetic nanonetworks in the terahertz band," in *2011 IEEE international conference on communications (ICC)*. IEEE, 2011, pp. 1–6.

[17] J. M. Jornet, "Low-weight error-prevention codes for electromagnetic nanonetworks in the terahertz band," *Nano Communication Networks*, vol. 5, no. 1-2, pp. 35–44, 2014.

[18] V. Petrov, D. Moltchanov, and Y. Koucheryavy, "On the efficiency of spatial channel reuse in ultra-dense thz networks," in *2015 IEEE Global Communications Conference (GLOBECOM)*. IEEE, 2015, pp. 1–7.

[19] ——, "Interference and sinr in dense terahertz networks," in *2015 IEEE 82nd Vehicular Technology Conference (VTC2015-Fall)*. IEEE, 2015, pp. 1–5.

[20] V. Petrov, M. Komarov, D. Moltchanov, J. M. Jornet, and Y. Koucheryavy, "Interference and sinr in millimeter wave and terahertz communication systems with blocking and directional antennas," *IEEE Transactions on Wireless Communications*, vol. 16, no. 3, pp. 1791–1808, 2017.

[21] R. Zhang, K. Yang, Q. H. Abbasi, K. A. Qaraqe, and A. Alomainy, "Analytical characterisation of the terahertz in-vivo nano-network in the presence of interference based on ts-ook communication scheme," *IEEE Access*, vol. 5, pp. 10 172–10 181, 2017.

[22] S. Cui, A. J. Goldsmith, and A. Bahai, "Energy-efficiency of mimo and cooperative mimo techniques in sensor networks," *IEEE Journal on selected areas in communications*, vol. 22, no. 6, pp. 1089–1098, 2004.

[23] A. Del Coso, U. Spagnolini, and C. Ibars, "Cooperative distributed mimo channels in wireless sensor networks," *IEEE Journal on Selected Areas in Communications*, vol. 25, no. 2, pp. 402–414, 2007.

[24] R. Y. Mesleh, H. Haas, S. Sinanovic, C. W. Ahn, and S. Yun, "Spatial modulation," *IEEE Transactions on vehicular technology*, vol. 57, no. 4, pp. 2228–2241, 2008.

[25] F. Berrahma, K. Ghanem, M. Nedil, and H. Bousbia-salah, "A novel multi-user spatial modulation-based code division multiple access scheme," in *2019 IEEE International Symposium on Antennas and Propagation and USNC-URSI Radio Science Meeting*. IEEE, 2019, pp. 1587–1588.

[26] N. Serafimovski, A. Younis, R. Mesleh, P. Chambers, M. Di Renzo, C.-X. Wang, P. M. Grant, M. A. Beach, and H. Haas, "Practical implementation of spatial modulation," *IEEE Transactions on Vehicular Technology*, vol. 62, no. 9, pp. 4511–4523, 2013.

[27] W. Belaoura, K. Ghanem, M. A. Imran, A. Alomainy, and Q. H. Abbasi, "A cooperative massive mimo system for future in vivo nanonetworks," *IEEE Systems Journal*, 2020.

[28] N. Serafimovski, S. Sinanović, A. Younis, M. Di Renzo, and H. Haas, "2-user multiple access spatial modulation," in *2011 IEEE GLOBECOM Workshops (GC Wkshps)*. IEEE, 2011, pp. 343–347.

[29] Y. Liu, L.-L. Yang, and L. Hanzo, "Spatial modulation aided sparse code-division multiple access," *IEEE Transactions on Wireless Communications*, vol. 17, no. 3, pp. 1474–1487, 2017.

[30] O. Sushko, "Terahertz dielectric study of bio-molecules using time-domain spectrometry and molecular dynamics simulations," Ph.D. dissertation, Queen Mary University of London, 2014.

[31] T. D. Dorney, R. G. Baraniuk, and D. M. Mittleman, "Material parameter estimation with terahertz time-domain spectroscopy," *JOSA A*, vol. 18, no. 7, pp. 1562–1571, 2001.

[32] M. Fukuma and K. Ishii, "Space-time code division multiple access based on spatial modulation," in *2015 IEEE 82nd Vehicular Technology Conference (VTC2015-Fall)*. IEEE, 2015, pp. 1–5.

[33] R. Mesleh, H. Haas, C. Ahn, and S. Yun, "Spatial modulation-ofdm," in *Proc. of the International OFDM Workshop*, 2006, pp. 30–31.

[34] M. Di Renzo, H. Haas, and P. M. Grant, "Spatial modulation for multiple-antenna wireless systems: A survey," *IEEE Communications Magazine*, vol. 49, no. 12, pp. 182–191, 2011.

[35] J. Mietzner, R. Schober, L. Lampe, W. H. Gerstacker, and P. A. Hoeher, "Multiple-antenna techniques for wireless communications-a comprehensive literature survey," *IEEE communications surveys & tutorials*, vol. 11, no. 2, pp. 87–105, 2009.

[36] M. Renzo, H. Haas, A. Ghrayeb, L. Hanzo, and S. Sugiura, "Spatial modulation for multiple-antenna communication," 2016.